Reprinted from JOURNAL OF APPLIED PHYSICS, Vol. 34, No. 8 2330–2336, August 1963

Printed in U. S. A.

Compressibility of Solids and Liquids at High Pressures

MELVIN A. COOK AND LEO A. ROGERS*
Institute of Metals and Explosives, University of Utah, Salt Lake City, Utah

(Received 30 November 1962)

An equation for compressibility (identical in form to the Tait equation) derived previously from the virial theorem and the Fermi–Thomas atomic model is modified on the assumption that one of its parameters ($a\beta_0$) is reciprocally related to the *internal pressure* when the *cohesive energy density* is assumed to be an essential part of the internal pressure. Pressure–volume data for about fifty homonuclear solids, two alloy systems, twenty ionic compounds, and five secondary bonded liquids are analyzed and the model found to fit with surprising accuracy when due consideration is given to pressure-induced phase or polymorphic changes and thermodynamic "holes" (most important near, and above, the melting point) that may contribute appreciably to specific volume. Data from static and shock methods of compression are considered and the differences noted. The model is apparently applicable to the compression of homonuclear solids and liquids, if indeed not all condensed materials in general.

INTRODUCTION

BY application of the virial theorem and the Fermi–Thomas model, the following equations were derived[1] for thermal expansion and compressibility of homonuclear solids:

$$\alpha/3=\alpha'=C_v/2\bar{T}_1, \tag{1}$$

$$\beta=9R(M/\rho)^{\frac{2}{3}}N^{\frac{1}{3}}/4\bar{T}, \tag{2}$$

where α = bulk thermal-expansion coefficient, α' = linear thermal-expansion coefficient, β = compressibility, $\bar{T}$ = average effective kinetic energy, $\bar{T}_1$ = average kinetic energy in the valence orbital, C_v = heat capacity, R = bond distance, ρ = density, M = atomic weight, and N = Avogadro's number. The basic idea was simply that the Fermi–Thomas (or particle in a box) model, which implies a definite relationship between the average kinetic energy and the density $[\bar{T}=f(\rho)]$, could be used to describe changes in solids. Thus, in treating thermal expansion the energy

$$H=\int_0^T C_v dT$$

was considered to lower the average kinetic energy by H. Since the total energy E is negative, a positive energy H decreases $|E|$. The virial theorem was used to relate $\bar{T}$ and E. For compressibility, on the other hand, the work of compression should increase $\bar{T}$ by $-(\frac{3}{2})RFN$, where F is the average force applied on each of the bonds.

The theory was considered to explain only the contribution to density changes from lattice parameter changes, and did not include those changes attributed to thermodynamic defects. For example, the contribu-

---

* Present address: Corning Glass Works, Corning, New York. This article comprises part of the dissertation submitted by Leo A. Rogers to the Graduate School, University of Utah in partial fulfillment of the requirements for the Doctor of Philosophy degree, June 1962.

[1] M. A. Cook, Discussions Faraday Soc. **22**, 203 (1956); "Properties of Solids," Bulletin No. 53, University of Utah, September 1951; J. Appl. Phys. 30, 725 (1959); *The Science of High Explosives* (Reinhold Publishing Corporation, New York, 1958), Chap. 9.

tion to the volume ($\Delta v'$) from Schottky-type defects according to Mott and Gurney[2] is given approximately by

$$\Delta v' = R^3 N \gamma B e^{-w_0/kT} \tag{3}$$

(see Ref. 2 for definition of constants γ, B, and w_0). For solids $\Delta v'$ should become appreciable only at temperatures approaching the melting point. It may be neglected at room temperature in solids having high cohesive energies and melting points.

The kinetic energy of the valence orbital $[\bar{T}_1 = f(\rho_1)]$ was assumed to be given approximately by the Fermi–Thomas equation

$$\bar{T}_1 = (h^2/2m)(3\rho_1/8\pi)^{\frac{2}{3}}, \tag{4}$$

where h = Planck's constant, m = electron mass, and ρ_1 was assumed to vary directly as the density of the atom. For all the other electrons, the kinetic energy $\bar{T}_i = f(\rho_i)$ ($\bar{T}_i$ the kinetic energy of the ith electron) was assumed to obey this "particle in a box" equation, or in other words, the ρ_i's being determined by the Fermi–Thomas "orbital size" equation. However, the ρ_i's were not all considered to change in the same proportion as energy H was added to or taken from the system. In thermal expansion the only appreciable change considered was that in the valence electrons, since electrons in filled bands would not be excited thermally. In compression, on the other hand, the kinetic energy was assumed to change in proportion to the "surface area" of the orbital computed on the basis of spherical charge distributions and the ratio $\bar{T}_i/\bar{T}_1$. Thus, all orbitals were considered to contribute to the "hardness" of an atom in proportion to $\bar{T}_1/\bar{T}_i$. This crude approximation proved inaccurate in describing the distribution of the applied force among the (Z) electron orbitals. That is, it led to values of effective average kinetic energy as a function (ϕ) of the kinetic energy of the valence orbital ($\bar{T} = \phi \bar{T}_1$) sometimes considerably in error based on the variance between calculated and experimental compressibilities. It may still be assumed, however, if the Fermi–Thomas model applies, that changes in the $\bar{T}_i$'s for compression of the atom are all related to the kinetic energy of the valence orbital, such that $\bar{T} = f(\rho)$ and also $\phi = g(\rho)$. This assumption alone permits integration of the last term or pressure coefficient of compressibility in the equation

$$\beta = \beta_0 + \int_0^p \frac{d\beta}{dp} dp. \tag{5}$$

Differentiation of Eq. (2) with $N^{\frac{1}{3}}R(m/\rho)^{\frac{1}{3}}$ replaced by a constant times the specific volume (v) gives the result

$$\frac{d\beta}{dp} = \beta\left[\frac{d\ln v}{dp} - \frac{d\ln\bar{T}}{dp}\right] = -\beta^2\left[1 - \frac{d\ln\bar{T}_1}{d\ln v} - \frac{d\ln\phi}{d\ln v}\right]. \tag{6}$$

Based on Eq. (4) the term $-d\ln\bar{T}_1/d\ln v$ becomes just $\frac{2}{3}$. Then with the additional assumption that $\bar{T}_i \neq f(v)$ for $i \geqslant 2$, one obtains $-d\ln\phi/d\ln v = b = \frac{2}{3}(1-1/\phi)$. This was the basis for the original derivation of $a = (5/3)+b$. However, this assumption is clearly in error, and the theory for a should thus be modified. For example, $\bar{T}$ should vary as θ_D, the Debye characteristic temperature, and, therefore, $-d\ln\bar{T}/d\ln v = \gamma$, the Grüneisen constant. Thus while the previous derivation of b gives $b \leqslant \frac{2}{3}$, the result should instead be $\gamma - \frac{2}{3}$, or about 1.3. Therefore, we shall here replace the questionable assumption about the constant value of ϕ by the alternate assumption $\bar{T} = f(v)$, such that from Eq. (4) one obtains $\phi = g(v)$ which leads to the result that b is a constant. Equation (6) then becomes

$$d\beta/dp = -\beta^2(1+\tfrac{2}{3}+b) = -a\beta^2, \tag{7}$$

where $a = (5/3)+b$. Combining Eqs. (5) and (7) and integrating successively by parts one obtains

$$\beta = \beta_0 \sum_{i=0}^{\infty} (-a\beta_0 p)^i = \beta_0/(1+a\beta_0 p). \tag{8}$$

[More simply, differentiate Eq. (8) to get Eq. (7).] We shall, however, use an alternate method described below to evaluate a from which b is obtained. Equation (8) has the same form of the Tait equation

$$\beta = C/(L+p), \tag{9}$$

and would be identical to it if the constants C and L were defined by a^{-1} and $(a\beta_0)^{-1}$, respectively.

The original model was intended to apply without the use of empirical constants by providing theoretically computed values of a. Unfortunately, the theory for a proved inadequate giving theoretical values in the range $1.8 < a < 2.3$, while actual values required to give the correct β's fell in the range $1.8 < a < 6$. Moreover, the required a's averaged about 3.0 which is greater than the upper limit of a permitted by the theoretical approximation in Ref. 1. It is the purpose of this article to modify the theoretical basis for a and to show that the improved model provides a reliable model for the high pressure compressibility of solids, if indeed not all condensed materials in general.

MODIFIED THEORY OF "a"

The proposed modification of the theory of a is based on the fact that Eq. (8) is of the form of the successful Tait equation, and that the L in the Tait equation has already been interpreted (although somewhat intuitively) as an internal pressure.[3–5] Thus, it is here postulated that for homonuclear solids

$$L = (a\beta_0)^{-1} = p_i, \tag{10}$$

---

[2] N. F. Mott and R. W. Gurney, *Electronic Processes in Ionic Crystals* (Oxford University Press, New York, 1953), p. 31.

[3] A. Wohl, Z. Physik. Chem. 99, 234 (1921).

[4] A. Carl, Z. Physik. Chem. 101, 238 (1922).

[5] R. Ginell, J. Chem. Phys. 35, 1776 (1961).

where p_i is the internal pressure generalized to include both the usual thermodynamic internal pressure $(\partial E/\partial v)_T$ and the *cohesive energy density* (p_i') given by the relation

$$p_i'=\epsilon_0/v_0, \tag{11}$$

where ϵ_0 is the cohesive energy at absolute zero. The internal pressure as used in this study is, therefore, defined by

$$p_i=(\partial E/\partial v)_T+\epsilon_0/v_0=(a\beta_0)^{-1}. \tag{12}$$

The ratio of density (or specific volume) at pressure p to that at atmospheric pressure is found by combining Eqs. (12) and (8) with the definition of compressibility ($\beta=-d\ \ln v/dp$) to give the result

$$\rho_0/\rho=v/v_0=(1+p/p_i)^{-1/a}. \tag{13}$$

Usually $\epsilon_0/v_0 \gg (\partial E/\partial v)_T$; and, therefore, for evaluating this model, p_i is approximated by $p_i'=p_i$. This is similar to ignoring $\Delta v'$ as given by Eq. (3).

Equation (13) predicts that plots of $\log(v/v_0)$ against $\log(1+p/p_i)$ should give straight lines of slope $-1/a$ $=\epsilon_0\beta_0/v_0$. Before evaluating this prediction, it is of interest to relate the present derivation to the Grüneisen constant, as expressed by

$$\gamma=\alpha v_0/\beta C_v. \tag{14}$$

From Eqs. (14), (1), and (2), one can obtain

$$\gamma=2\phi/3. \tag{15}$$

In the Grüneisen derivation γ is also given by

$$\gamma=-d\ \ln\nu_m/d\ \ln v, \tag{16}$$

where ν_m is the characteristic frequency of the vibrational modes of the solid. Since only vibrational energy is involved in H for thermal expansion of homonuclear solids (except near absolute zero and high temperatures where free electrons contribute appreciably to heat content), $\bar{T}$ should vary directly as ν_m, such that

$$\gamma=\frac{d\ \ln\nu_m}{d\ \ln v}=-\frac{d\ \ln\bar{T}_1}{d\ \ln v}-\frac{d\ \ln\phi}{d\ \ln v}, \tag{17}$$

which gives the result

$$a=1+2\phi/3=1+\gamma. \tag{18}$$

APPLICATIONS TO HOMONUCLEAR SOLIDS

Plots of $\log(v/v_0)$ against $\log(1+p/p_i)$ were made for many metals, alloys, and other homonuclear solids where data were available. The majority of data gave straight line plots satisfying the linearity criterion with excellent precision. Two types of (expected) irregularities were noted and explained.

(1). In the alkali metals, for example, straight line plots were obtained only at high pressure, deviations from linearity being prominent at low pressures. The log–log plot for sodium (Fig. 1) deviated from linearity in the range $p<12$ kbars, but was linear for $p>12$ kbars. In this case the linear part of the curve extrapolates to zero pressure at about $v/v_0=0.92$ indicating a $\Delta v'/v$ contribution of about 0.08. All of the alkali metals are characterized by low cohesive energies and melting points, and have a significant contribution of thermodynamic defects according to Eq. (3). The energy required to form a hole should increase with pressure, however, according to the relation

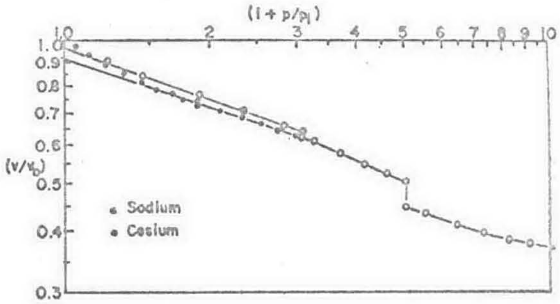

FIG. 1. Log–log plot for isothermal compression of sodium and cesium. Data from Ref. 6.

$$w_0=w_0^0+pR^3,$$

where pR^3 is the extra work required to form a hole of volume R^3 at pressure p over that at $p=0$. Other homonuclear solids that exhibited nonlinear log–log plots were sulfur, tellurium, and some of the rare earths. Most of these have low melting points, and thus an appreciable $\Delta v'/v$ contribution at ambient conditions. Mercury, on the other hand, exhibited only a straight line log–log plot despite its very low melting point. In some cases gradual structure changes may also contribute to deviations from linear log–log plots.

(2). Sharp pressure-induced phase (or polymorphic) transitions caused first-order discontinuities in the log–log plots. Bismuth and cesium (Figs. 1, 5, and 6) are examples of this. The fact that the log–log plots are straight lines on either side of the transition is striking evidence for the validity of the present model.

A few examples of the log–log plots are given in Figs. 1–6. Table I, however, summarizes the information obtained from plots made for all homonuclear solids where data were available. The experimental $p(v)$ data

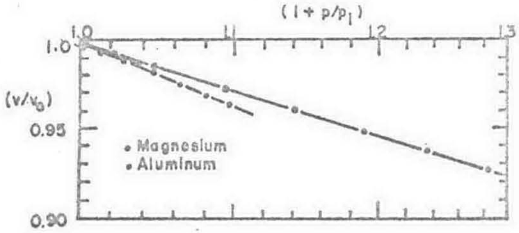

FIG. 2. Log–log plot for isothermal compression of magnesium and aluminum. Data from Ref. 6.

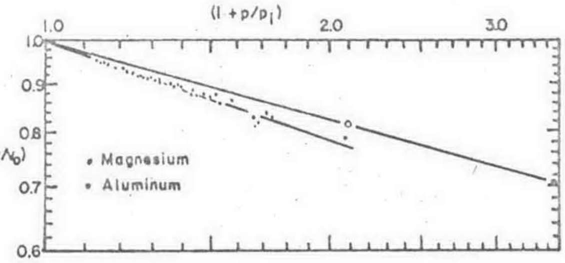

FIG. 3. Log–log plot for shock compression of magnesium and aluminum. Data from Refs. 8 and 9.

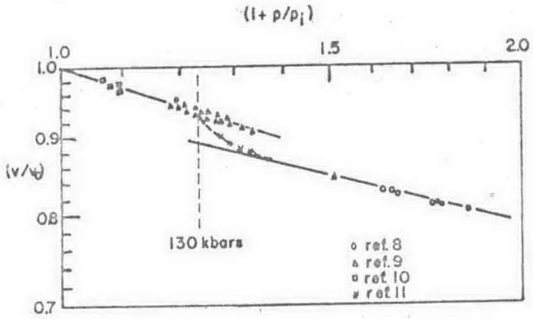

FIG. 4. Log–log plot for shock compression of iron. Data from Refs. 8, 9, 10, and 11.

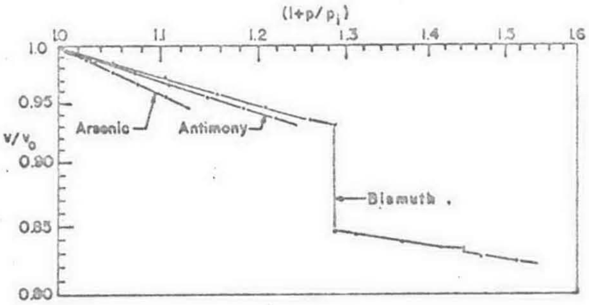

FIG. 5. Log–log plot for osothermal compression of arsenic, antimony, and bismuth. Data from Ref. 6.

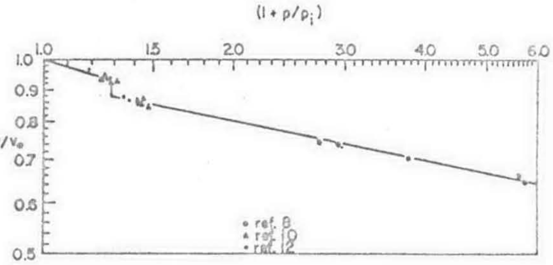

FIG. 6. Log–log plot for shock compression of bismuth. Data from Refs. 8, 10, and 12.

were taken from Bridgman[6] (static pressure data), and from the brilliant work pioneered at Los Alamos using dynamic (shock) methods.[7–15] Data for ϵ_0 were taken from Seitz[16] and the Bureau of Standards.[17]

Values of a, found empirically from the slopes of the log–log plots of data obtained by the shock loading method, were an average of 15% higher than corresponding values for static compression, owing apparently to shock heating and other dissipative factors[18,19] that differentiate the shock process from the more common isothermal or adiabatic processes. The ratio of isothermal compressibility (β_T) to adiabatic compressibility (β_S) is found from thermodynamics to be

$$\beta_T/\beta_S = C_p/C_v. \tag{19}$$

Since C_p and C_v are nearly the same for solids, little difference should exist between isothermal and adiabatic compressibilities as compared to the larger difference between the isothermal and shock wave compressibilities. From Eq. (10) and the expected independence of p_i on the method used, one obtains

$$a_T\beta_{T0} = a_S\beta_{S0} = a_H\beta_{H0}. \tag{20}$$

Grüneisen Constants

A comparison of the γ's obtained from the a's and Eq. (18) with those obtained by more direct methods by Grüneisen,[20] Slater,[20] and Benedek[21] are given in Table II. Included in this comparison are results computed from Eq. (15) using the data previously derived by the approximate method given in Ref. 1. The favorable comparison of results indicates that the present theory of a is satisfactory. The γ's obtained from the ϕ's and Eq. (15) are apparently not seriously in error either, which implies that the approximation used previously to calculate ϕ was reasonably reliable, but the method of relating ϕ to a, which involved the change of ϕ with density, was seriously in error.

---

[6] P. W. Bridgman, *The Physics of High Pressures* (G. Bell and Sons, London, 1958); Proc. Am. Acad. Arts Sci. **74**, 21 (1940); **76**, 1, 9 (1945); **76**, 55, 71 (1949); **83**, 1 (1954); **84**, 131 (1957).

[7] R. W. Goranson, D. Bancroft, B. L. Burton, T. Blechar, E. E. Houston, E. Y. Gettings, and S. L. Landeen, J. Appl. Phys. **26**, 1472 (1955).

[8] M. H. Rice, R. G. McQueen, and J. M. Walsh, Solid-State Phys. **6**, 1 (1958).

[9] S. Katz, D. R. Curran, and D. G. Doran, "Hugoniot Equation of State of Aluminum and Steel from Oblique Shock Measurement," Poulter Labs Tech. Report 025-57 (1957), Stanford Research Institute, Menlo Park, California.

[10] D. S. Hughes, L. E. Gourley, and M. F. Gourley, J. Appl. Phys. **32**, 624 (1961).

[11] D. Bancroft, E. L. Peterson, and F. S. Minshall, J. Appl. Phys. **27**, 1207 (1956).

[12] R. E. Duff and F. S. Minshall, Phys. Rev. **108**, 1207 (1955).

[13] J. M. Walsh and M. H. Rice, J. Chem. Phys. **26**, 818 (1957).

[14] M. A. Cook, R. T. Keyes, and W. O. Ursenbach, J. Appl. Phys. **33**, 3413 (1962).

[15] O. C. Trulson, D. E. Hudson, and F. H. Spedding, J. Chem. Phys. **35**, 1018 (1961).

[16] F. Seitz, *The Modern Theory of Solids* (McGraw-Hill Book Company, Inc., 1940).

[17] U. S. Bureau of Standards, *Selected Values of Chemical Thermodynamic Properties* (U. S. Govt. Printing Office, Washington, D. C., 1952).

[18] R. H. Wentorf, *Modern Very High Pressure Techniques* (Butterworths Scientific Publications, Ltd., London, 1962).

[19] G. R. Fowles, "Shock Wave Compression of Quartz," Ph.D. thesis, Stanford University (October 1961).

[20] C. Kittel, *Introduction to Solid State Physics* (John Wiley & Sons, Inc., New York, 1956).

[21] G. B. Benedek, Phys. Rev. **114**, 467 (1959).

TABLE I. Summary of information from $\log(v/v_0)$ vs $\log(1+p/p_i)$ plots.

					Straight-line sections		Discontinuities	
Metal	ϵ/v_0 (kbars)	a_T	a_H	$\Delta v'/v$	Isothermal compression[a]	Shock compression[a]	Isothermal compression[a]	Shock compression[a]
Cu	475	2.92	3.32	0.0	0–0.8†[b]	0.7 – 1.6†	none	none
Ag	278	3.74	4.33	0.0	0–1.2†	0.7 – 1.9†	none	none
Au	335	4.47	5.19	0.0	0–0.7†	0.5 – 1.1†	none	none
Li	116	1.89		0.07	0.3–0.9†		none	
Na	45	2.78		0.09	0.5–2.0†		none	
K	20	3.35		0.08	0.7–5.0†		none	
Rb	15	2.85		0.03	0.2–6.6†		none	
Cs	11	2.66		0.03	0.1–2.1 2.1–4.1†		2.1 (small) 4.1 (large)	
Be	641	1.79	2.32	0.0	0–0.17†	0.2 – 1.5†	none	none
Mg	101	3.69	3.98	0.0	0–0.28†	1.1 – 2.4†	none	none
Zn	141	5.01	5.54	0.0	0–0.28†	1.4 – 3.3†	none	none
Cd	43	11.0		0.0	0–0.53†	5.3 –11†	none	
Hg	42	7.18	7.41	0.0	0–0.28†	5.3 –11†	none	none
Al	309	2.44	3.00	0.0	0–0.1†	0.13– 3.3†	none	none
La	162	1.83		0.0	0–0.14 0.14–0.25†		0.14 (slight)	
In	154	2.89	4.09	0.01	0.18–0.32†	2.0 – 4.3†	none	none
Tl	104	4.89		0.0	0–0.24†	1.4 – 2.7†	none	
Ti	458	2.18	2.94	0.0	0–0.04 0.04–0.09†	0.4 – 0.9†	0.04 (change in slope)	none
Zr	370	2.32		0.0	0–0.06 0.06–0.11†	0.6 – 1.1†	0.06 (change in slope)	
Sn	184	3.05	4.61	0.05	0–0.16†	1.0 – 2.3†	none	none
Pb	106	4.08	4.96	0.0	0–0.95†	2.0 – 4.8†	none	none
As	192	2.42		0.0	0–0.21†		none	
Sb	137	3.56		0.0	0–0.21†		none	
Bi	97	3.47		0.0	0–0.28 0.28–0.52†	0.2 – 0.28 0.28– 4.8†	0.28 (large)	0.28
Fe	565	2.99		0.0	0–0.05†	0.1 – 0.25 0.4 – 0.8†	none	0.25–0.4
Co	660	2.90	3.44	0.0	0–0.05†	0.38– 0.75†	none	none
Ni	636	2.90	3.28	0.0	0–0.05†	0.38– 0.85†	none	none
Ru	797	3.62		0.0	0–0.04†		none	
Rh	692	3.73	4.32	0.0	0–0.05†	0.4 – 0.8†	none	none
Pd	434	4.20	4.57	0.0	0–0.77†	0.6 – 1.4†	none	none
Ta	704	2.90		0.0	0–0.05†		none	
Nb	709	2.49	2.69	0.0	0–0.05†	0.33– 0.75†	none	none
Mo	685	3.83	3.94	0.0	0–0.05†	0.38– 0.8†	none	none
W	877	3.48		0.0	0–0.04†		none	
Cr	459	4.20	4.31	0.0		0.55– 1.05†		none
Ir	798	4.31		0.0	0–0.04†		none	
Pt	560	4.74	4.78	0.0	0–0.06†	0.54– 1.0†	none	none
Gd	180	2.45		0.0	0–0.2†		none	
Ho	165	2.62		0.0	0–0.2†		none	
Pr	173	1.80		0.0	0–0.2†		none	
Ce	170	0.9		0.0	0–0.06†		0.08?	
Non-metals								
Si	301	3.85		0.0	0–0.1†		none	
Ge	240	3.60		0.0	0–0.13†		none	
Te	96	2.58		0.03	0.15–0.4 0.4 –0.53†		0.4 (large)	
S	143	2.81		0.12	0.35–0.7†		none	

[a] In terms of p/p_i.

[b] † denotes upper limit of experimental data.

TABLE II. Comparison of Grüneisen constants obtained by different investigators.

Metal	Grüneisen[a]	Slater[a]	Benedek[b]	Cook[c,d]	This study[e] a_T
Copper	1.96	1.63	1.9	1.94	1.92
Silver	2.40	2.2	2.5	2.40	2.74
Sodium	1.25	1.50	···	···	1.78
Potassium	1.34	2.52	···	···	2.35
Aluminum	2.17	2.32	···	···	1.44
Manganese	2.42	5.5	···	1.63	2.4
Iron	1.60	1.4	1.68	···	1.99
Cobalt	1.87	1.8	2.1	···	1.90
Nickel	1.88	1.9	2.2	···	1.90
Platinum	2.54	3.0	3.3	···	3.74
Palladium	···	···	2.5	···	3.20
Tungsten	···	···	1.7	···	2.48

[a] See Ref. 18.
[b] See Ref. 19.
[c] See Ref. 1.
[d] Using computed ϕ's and Eq. (15).
[e] From Eq. (18) and a_T data taken from the log–log plots.

Compressibilities

Table III presents a comparison of observed compressibilities with those obtained from the slopes of the log–log plots and the equation

$$\beta_0 = v_0/a\epsilon_0 \qquad (21)$$

obtained by combining Eqs. (10) and (11). The agreement is quite good. Elements such as sodium in which $\Delta v'$ is appreciable were not included in this comparison, since a direct comparison is possible only when the log–log plots extrapolate to $v/v_0=1$ at $p=0$.

ALLOYS

Figure 7 presents $\log v/v_0$ against $\log(1+p/p_i)$ plots for the Cu–Ni and Ag–Pd alloys. The internal pressure was calculated from the relation

$$p_i = (\textstyle\sum_i \epsilon_{0i} + \Delta\epsilon)/v_0, \qquad (22)$$

where $\Delta\epsilon$ is the energy of solution or reaction, and v_0 is the molar volume of the alloy. For the Cu–Ni system, the slopes of the log–log plots were essentially equal for the pure metals with $\Delta\epsilon$ and the change in molar volumes being negligible. Thus, all the data from the Cu–Ni system fell, as expected, on the same $\log(v/v_0)$ against $\log(1+p/p_i)$ plot.

TABLE III. Theoretical vs observed β_0's for metals.

Metal	β_0 (calc.)[a]	β_0 (obs.)[a]	Metal	β_0 (calc)[a]	β_0 (obs.)[a]
Be	8.72	8.55	Pd	5.50	5.28
Mg	25.6	29.5	Pt	3.78	3.60
La	33.7	35.1	Cu	7.22	7.19
Ti	10.5	7.97	Ag	9.62	9.87
Zr	11.6	11.0	Au	6.00	5.77
Nb	5.66	5.7	Cd	21.	18.
Ta	4.90	4.97	Al	13.2	13.4
Mo	3.81	3.61	In	22.4	25.0
W	3.28	3.18	Tl	19.7	27.7
Fe	5.94	5.87	Si	8.6	3.1
Ru	3.46	3.72	Ge	11.6	13.8
Co	5.32	5.39	Pb	23.1	23.7
Rh	3.84	3.72	Bi	27.2	29.2
Ir	2.80	2.68			
Ni	5.42	5.29			

[a] Expressed in units of kbars$^{-1}\times10^4$.

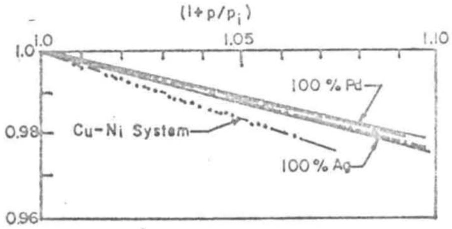

FIG. 7. Log–log plot for isothermal compression of the Cu–Ni and Ag–Pd alloy systems. Data from Ref. 6.

For the Ag–Pd system, log–log plots for the pure metals were different, and the log–log plots for the alloys thus fell between those for the pure metals, and an approximate linear relationship was found between the value of a and the composition. For ideal alloys a linear relationship between composition and a would be expected, but systems where $\Delta\epsilon$ and changes in molar volume are appreciable should exhibit a more complicated relation between a and composition.

HALIDES

Figures 8 and 9 present log–log plots for some halides. While in the silver halides these plots were linear all the way, with discontinuities due to phase changes, in the alkali halides the linearity criterion was not observed in all cases.

LIQUIDS

Figure 10 presents the log–log plot for water using shock-loading data. The log–log plot is nonlinear in the region $0<p/p_i<0.5$, and linear for $p/p_i>0.5$. The extrapolation of the straight line section to zero pressure yielded a $\Delta v'/v$ contribution of 0.14. This volume frac-

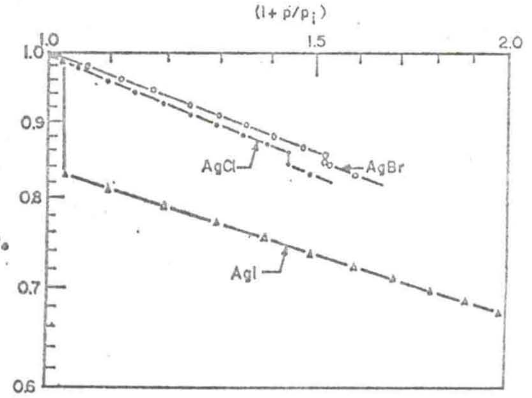

FIG. 8. Log–log plot for isothermal compression of some silver halides. Data from Ref. 6.

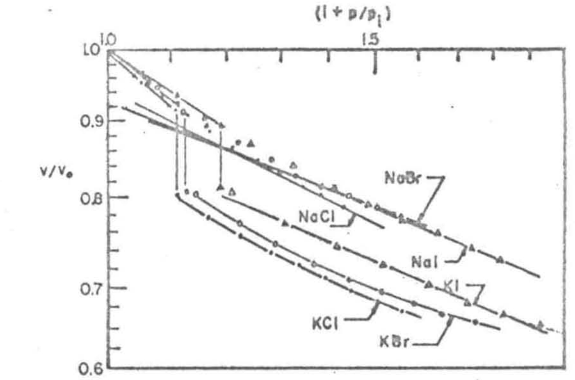

FIG. 9. Log–log plot for isothermal compression of some alkali halides. Data from Ref. 6.

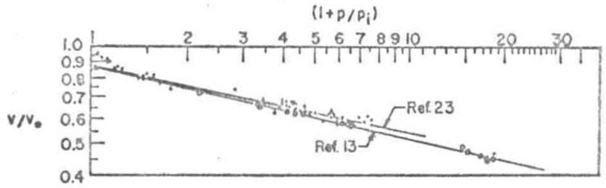

FIG. 10. Log–log plot for shock compression of water. Data from Refs. 13 and 23.

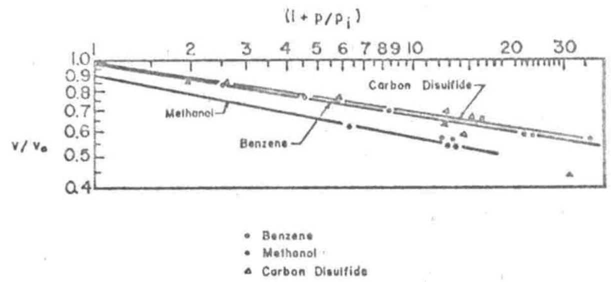

FIG. 11. Log–log plots for shock compression of several liquids. Data from Ref. 13 and Table IV.

tion of void space in the liquid is in excellent agreement with the Eyring theory of holes in liquids.[22]

Figure 11 presents log–log plots for methanol, benzene, and carbon disulfide. Additional shock compression data, using the aquarium method,[14] were obtained in this study, and the results are given in Table IV along with those obtained from the log–log plots. Again, straight lines characterized the log–log plots at high pressures.

TABLE IV.

A. Experimental data for shock compression of four liquids.

Liquid	Shock velocity km/sec	Particle velocity km/sec	p kbars	v/v_0
Methyl alcohol	5.50	2.46	107	0.552
	5.30	2.30	96	0.566
	5.34	2.42	102	0.546
Carbon tetrachloride	4.20	1.93	129	0.542
	3.29	1.36	72	0.588
	2.85	1.10	50	0.614
	2.18	0.605	21	0.712
	1.93	0.390	12	0.798
Benzene	4.59	1.92	78	0.581
	4.59	1.88	74	0.590
	3.16	0.980	25	0.690
	2.77	0.670	16	0.758
	2.47	0.560	12	0.774
	1.97	0.28	4.8	0.858
Carbon disulfide	3.83	1.28	62	0.666
	3.75	1.46	67	0.610
	3.63	1.12	51	0.692
	3.29	1.21	50	0.632
	3.18	1.68	43	0.660
	2.70	0.63	21	0.767
	1.91	0.30	7.3	0.843
	1.90	0.28	7.0	0.853
	1.65	0.19	4.0	0.885

B. Information for log–log plots of liquids used. (See Fig. 11.)

Liquid	p_i (kbars)	$\Delta v'/v_0$	a_H[a]
H_2O	24.3	0.15	4.4
CCl_4	3.07	0.11	7.9
CS_2	4.40	0.02	5.6
C_6H_6	3.44	0.03	6.1
CH_3OH	8.68	0.10	5.1

[a] High-pressure region where straight-line results.

Murnaghan Equation Comparison

Finally, it is of interest to compare Eq. (13) to the Murnaghan equation of state[23] derived from finite strain theory, namely,

$$v_0/v=[1+kp/(\lambda_0+\tfrac{2}{3}\mu_0)]^{1/k}, \tag{23}$$

where λ_0 and μ_0 are the Lamé elastic constants, and k is a constant which was assumed to be $\frac{1}{3}$ from the "(drastic) assumption that λ and μ are independent of p_0." Equation (23) becomes identical with Eq. (13) if one assumes that $a=1/k$ and $p_i=(\lambda_0+\frac{2}{3}\mu_0)/k$. Murnaghan also points out that as $v\rightarrow\infty$, $p\rightarrow-(\lambda_0+\frac{2}{3}\mu_0)/k$, and that the medium in theory would support a hydrostatic tension of $(\lambda_0+\frac{2}{3}\mu_0)/k$ before rupture. This is the force required to overcome the cohesive forces of the medium, and one can conclude that the assumption of $p_i=\epsilon_c/v_0=(\lambda_0+\frac{2}{3}\mu_0)/k$ is not unreasonable. On the other hand, obtaining good workable values for k has presented some difficulty and empirical values are generally used. From the values of a given in Table I, one observes that the rough assumption of $k=\frac{1}{3}$ is quite good in many cases, but is also seriously in error for many cases compared to the present work. The fact that the present theory yields an equation of state of the same form as that of Murnaghan, however, lends support to the validity of the present theory.

---

[22] H. Eyring, B. J. Stover, E. M. Eyring, and D. J. Henderson, *Statistical Mechanics and Dynamics* (John Wiley & Sons, Inc., New York, to be published).

[23] F. D. Murnaghan, *Finite Deformation of an Elastic Solid* (John Wiley & Sons, Inc., New York, 1951).